Advancing Semiconductor Manufacturing through DNA-Templated Lithography and Molecular-Scale Patterning of 2D Materials

Anumita Kumari[1]
Deaprtment of chemistry
Univeristy of Pittsburgh
Pittsburgh, USA
ank239@pitt.edu

Michael Curtis[1]
Micron School of Materials Science and Engineering
Boise State University
Boise, USA
mikecurtis1@u.boisestate.edu

Arpan De[1]
Department of Electrical and Computer Engineering
University of Washington
Seattle, USA
arpan99@uw.edu

Haitao Liu
Deaprtment of chemistry
Univeristy of Pittsburgh
Pittsburgh, USA
hliu@pitt.edu

David Estrada
Micron School of Materials Science and Engineering
Boise State University
Boise, USA
daveestrada@boisestate.edu

M.P. Anantram
Department of Electrical and Computer Engineering
University of Washington
Seattle, USA
anantmp@uw.edu

[1] Authors had equal contribution

***Abstract*— This research paper explores the potential of MoS_2 in electronic devices. Monolayer Molybdenum disulphide(MoS_2) characterization reveals significant bilayer coverage with minimal out-of-plane growth, indicating low defect density, ideal for doping using DNA nanostructures. A simulation study using Quantum-Espresso DFT examines MoS_2 bandgap modulation due to counterion diffusion from DNA, highlighting the electron transfer mechanism during Lithium intercalation. Lastly, the study demonstrates stable deposition of DNA triangles and nanotubes on various MoS_2 surfaces, challenging previous stability reports and attributing enhanced stability to the structural robustness of DNA triangles and nanotubes. These findings collectively contribute valuable insights into advancing 2D electronics.**

Keywords—DNA origami, Molybdenum disulpide (MoS_2), 2D electronics, doping

I. Introduction

The exponential growth of integrated circuits, integral to modern technologies, has faced challenges in recent years due to the increasing difficulty of lithographically patterning silicon with a pitch smaller than 25 nm using optical lithography. This limitation has spurred focused research on engineering innovative materials and patterning methods for electronic devices. The current reliance on Si-electronics poses significant challenges in terms of scalability, underscoring the critical necessity for a new material system in electronics.

In semiconductor manufacturing's dynamic landscape, this research pioneers the integration of molecular-scale patterning and doping into atomically thin materials like graphene and MoS_2, utilizing DNA-templated lithography masks. Overcoming challenges in traditional lithography (sub-25 nm pitch) and addressing the quest for a new computing paradigm, 2D materials emerge as candidates for 21st-century electronics.

Liu and Xiong have recently introduced an innovative technique for silicon (Si) doping, utilizing DNA nanostructures as a dopant source[1]. Through their method, they demonstrated that, under elevated temperatures, phosphorus atoms from the DNA diffuse into the silicon wafer, leading to the creation of n-doped regions. The spatial distribution of dopant atoms is determined by the shape of the DNA nanostructure, showcasing sub-50 nm resolution in their experiments. Utilizing individually doped regions, field-effect devices were successfully fabricated, confirming the effectiveness of their n-doping approach. On other hand, in prior experiments, Liu observed the co-deposition of positively charged counter ions (e.g., Mg^{2+}) when depositing a DNA nanostructure on a solid substrate. Remarkably, the shape of these DNA nanostructures remains unchanged even under harsh conditions, such as heating to 200 °C, showcasing their enhanced stability compared to solution counterparts[2]. Importantly, even after removing DNA nanostructures through thermal or UV-Ozone oxidation, the counter ions persist undisturbed on the substrate. Using these, Our hypothesis is that DNA nanostructure can assemble ionic intercalants and deliver these ions to a 2D material surface with nanometer precision.

Here, we have shown preliminary results that indicate the proposed DNA based controlled doping technique in 2D materials offers a lot of promises

II. Experimental

A. Monolayer MoS_2 synthesis

Molybdenum hexacarbonyl and hydrogen sulfide were used as precursors and deposited on c-plane sapphire by metal organic chemical vapor deposition (MOCVD). The MOCVD system used is composed of a cold walled quartz tube chamber with an inductively heated SiC-coated graphite susceptor that produces fully coalesced transition metal dichalcogenide films (TMD) across a 2-inch wafer. The susceptor features gas foil rotation to ensure sample uniformity across the entirety of the

wafer. The growth process consists of a pre deposition anneal step in a hydrogen atmosphere and minimal flow of the hydride precursor. This step forms ordered terraces on the sapphire surface while also stripping dangling oxygen bonds on the wafer surface. The dilute amounts of sulfur can also fill vacancies on the sapphire basal plane. All this contributes to a more controlled nucleation of the 2D material. After the pre-anneal step the metalorganic precursor is introduced to start nucleation and growth. Once the growth is complete a post growth anneal is conducted again using the hydride precursor and hydrogen carrier gas. This step allows for vacancy filling in the TMD basal plane. Upon removal from the reaction chamber, we characterize the coverage and quality of the deposited films. Atomic Force Microscopy (AFM) is used to determine layer coverage. Monolayer coalescence is confirmed using Raman spectroscopy, where the separation of the two prominent Raman modes correlate to the characteristic in plane and out of plane vibrations of the layer. The separation of these two peaks directly correlates to the layer number of the deposited sample[3], [4]. Additional layers can then be visualized by AFM. Quantification of layer coverage above the monolayer is accomplished by an image processing technique using FIJI. In this technique the AFM image is converted to grayscale and methodically segmented into bins. The resulting histogram is used to generate a binary mask using an ISO Data thresholding method, yielding a percent contribution to the total image.

B. Bulk and multilayer MoS_2 preparation

Fresh multilayer and bulk MoS_2 samples were prepared using MoS_2 crystals obtained from SPI supplies. For the bulk MoS2, the process involved utilizing scotch tape to peel thin layers from the MoS_2 crystal., while for multilayer MoS_2 (5-6 layers), a sequential peeling approach was employed. Specifically, a single tape was used to extract a thin layer from the MoS_2 crystal, followed by placing a fresh scotch tape on the previously used one and repeating the layer-peeling process several times. Multilayer MoS_2 was confirmed using AFM.

C. DNA origami synthesis, deposition on MoS_2 and doping

DNA triangle and DNA nanotube was synthesized based on previous report[5,6]. To study deposition of DNA origami on MoS_2, 20 uL (5 ug/mL) DNA triangle was deposited on MoS_2 and left undisturbed for 30 minutes. After 30 minutes the sample was washed with 90:10 Ethanol: water mixture and analyzed using AFM. Bulk MoS_2 samples were analyzed without washing. To confirm doping of MoS_2, kelvin probe force microscopy (KPFM) was used.

After the samples were dried using stream of N_2, the samples were kept in a furnace and heated to 500 °C for 1 hour and then imaged using KPFM to confirm the doping of MoS_2 with Mg^{2+}.

III. Result and Discussion

A. MoS_2 characterization

We observed ssignificant bilayer coverage occurs while achieving wafer scale coalescence with minimal multilayer (3+ layers) and out of plane growth. Out of plane growth occurs when nucleated domains grow into each other and begin growing normal to the basal plane rather than properly ripening into a smooth flat film. Samples used in this study averaged 27% Bilayer coverage with less than 2% multilayer/out of plane coverage. Raman spectroscopy is also used to get a qualitative understanding of the defect nature of the 2D material. 50 µm maps are taken at multiple points on the wafer surface. The characteristic in-plane and out-of-plane Raman peaks from the spectral maps are analyzed as well as checking for the presence of the defect associated LA(M) peak[7], [8]. Samples produced for this study lack this LA(M) peak which is evidence of a low defect density. This low defect density along with the limited amounts of multilayer regions indicate that these TMD samples have a pristine basal plane making them ideal candidates for doping ions using DNA nanostructures.

B. Simulation study of MoS2 bandgap modulation

When the DNAs are kept for a long period of time on the surface of 2D materials, counterions get diffused into the film, modulating its bandgap, subsequently leading to variation in transport properties. To study this band gap modulation, All the first-principal calculations have been carried out in Quantum-Espresso Density Functional Theory (DFT) package [9]. For all atoms, ultrasoft pseudopotentials have been used [10]. The 3×3 MoS_2 supercell without and with a single Lithium atom is shown in Figure 1(a) and (c) respectively. The first step in the simulation involves a gamma point relaxation of both the structures. Due to large size of the system and limited computational resources, relaxation has been done with a gamma point calculation. However, for the band calculations, we have chosen a highly dense K-mesh. The K-path for each structure has been computed according to [11,12]. Both force and electron convergence threshold for system optimization has been considered to be 1×10^(-5) eV/Å. A degauss value of 0.002 has been used. The energy cutoff is chosen to be 700 eV. To negate the impact of vertical supercell, a vacuum 20 Å is considered. From previous works [13], it is known that DFT cannot estimate the van-der Waals forces effectively, thus a van-der Waals correction model ('grimme-d3') [14] has been invoked in the simulation setup. The band structures of the system without and with Lithium are shown in Figure 1(b) and 2(d). It can be noticed that the Fermi energy lies almost in the middle for the case without

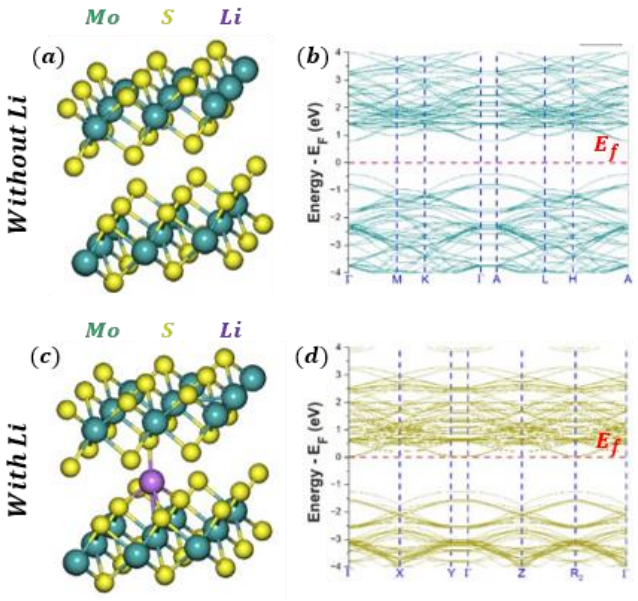

Fig. 1. 3×3 MoS2 supercell (a) without and (c) with Lithium (Li) intercalated atom leading to change in bandgap modulation as can be seen in (b) & (d) for the two cases. The Fermi energy (E_f) is shown in red dotted line. The K-path calculations has been computed according to [8]

any intercalation while it shifts towards the conductance band during Li intercalation. The reason can be attributed to the donation of electrons by Li atom. For deeper insights, we have performed a fat band analysis to understand the contribution of different orbitals in bandgap determination. It has been found that the d-orbitals of Molybdenum (Mo) and p-orbitals of Sulphur (S) contributes majorly while minor contribution comes from s-orbitals of Lithium (Li), asserting the transfer of electrons between Li and MoS_2 layer.

C. *DNA origami stability on MoS_2 and doping*

We observed stable DNA triangle and DNA nanotube deposition on monolayer, multilayer and bulk MoS_2 surfaces. The structures were confirmed by AFM and KPFM. Our results differ from the previously reported stability of DNA origami on MoS_2 [15]. The DNA origami used in their study was seen to undergo severe deformation after being deposited on freshly exfoliated MoS_2. We believe this is due to greater structural stability of DNA triangle and nanotube.

Initial KPFM imaging of DNA nanotube confirms its presence on potential image Figure 3(b). We have not yet been able to dope Mg^{2+} into MoS_2.

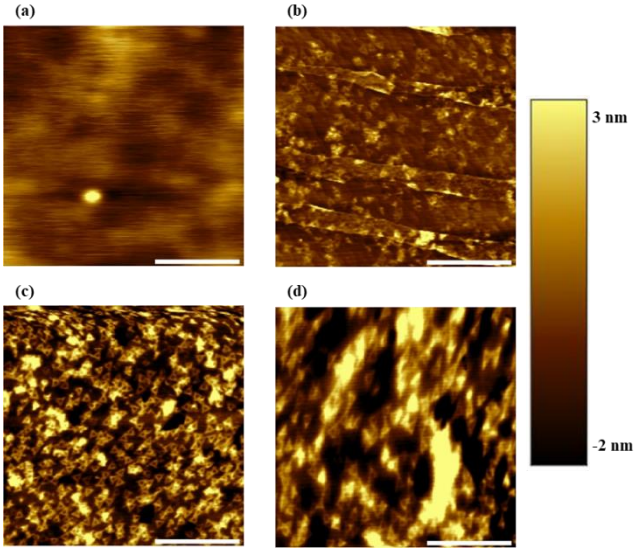

Fig. 2. AFM image showing DNA triangle deposited on different MoS_2 surfaces (a) monolayer MoS_2 (b) DNA triangle deposited on monolayer MoS_2 (c) DNA triangle deposited on bulk MoS_2 and (d) DNA triangle deposited on multilayer MoS_2. Scale indicates 1 µm

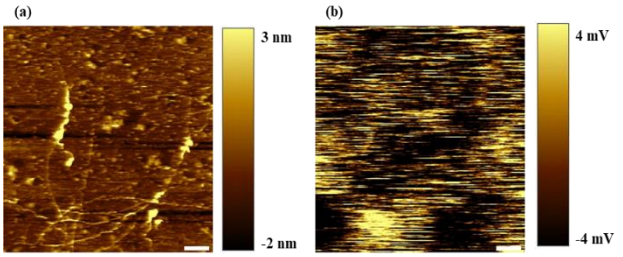

Fig. 3. KPFM image showing height trace and the potential trace of DNA nanotube deposited on Monolayer MoS_2 (a) Height trace of DNA nanotube deposited on monolayer MoS_2 (b) Potential trace of DNA nanotube deposited on monolayer MoS_2. Scale indicates 1 µm.

This work was funded by National Science Foundation

IV. Conclusion and Future Direction

In conclusion, these findings collectively contribute valuable insights into advancing 2D electronics. The successful synthesis and characterization of MoS_2, simulation study providing insights into bandgap modulation induced by counterion diffusion from DNA, emphasizing the electron transfer mechanism during Lithium intercalation, coupled with innovative DNA templating techniques, open avenues for the development of novel materials and methodologies in semiconductor manufacturing.

It is to be noted that the results reported here are only preliminary and we have plans for future experiments. We have not yet been successful in doping magnesium/metal cation into MoS_2. We plan on working towards this and confirm the doping of MoS_2 using KPFM. Although we believe these results can spur future experimental research, there are a lot of open questions that need to be addressed. For instance, we are working on improving the doping accuracy on MoS2 by considering several counterions. The choice of counterions mainly depends on DNA-binding strength and diffusion efficiency in MoS2 surface. From a computational standpoint, we plan to intercalate a variety of counterions to understand the level of MoS2 electrostatics. We also intend to increase the size of our system to negate the effect of very high doping density. The fat band analysis will be extended to a tight binding model to compute transport properties of these periodic systems.

References

[1] Bai, R.; Du, Y.; Xu, A.; Hu, Y.; Erickson, J. R.; Hui, L.; Chen, J.; Xiong, F.; Liu, H. DNA-Based Strategies for Site-Specific Doping. *Advanced Functional Materials* **2021**, *31*, 2005940.

[2] Kim, H.; Surwade, S. P.; Powell, A.; O'Donnell, C.; Liu, H. Stability of DNA Origami Nanostructure under Diverse Chemical Environments. *Chemistry of Materials* **2014**, *26*, 5265-5273.

[3] Li, H.; Zhang, Q.; Yap, C. C. R.; Tay, B. K.; Edwin, T. H. T.; Olivier, A.; Baillargeat, D. From Bulk to Monolayer MoS2: Evolution of Raman Scattering. *Advanced Functional Materials* **2012**, *22*, 1385-1390.

[4] Gołasa, K.; Grzeszczyk, M.; Bożek, R.; Leszczyński, P.; Wysmołek, A.; Potemski, M.; Babiński, A. Resonant Raman scattering in MoS2—From bulk to monolayer. *Solid state communications* **2014**, *197*, 53-56.

[5] Hung, A. M.; Micheel, C. M.; Bozano, L. D.; Osterbur, L. W.; Wallraff, G. M.; Cha, J. N. Large-area spatially ordered arrays of gold nanoparticles directed by lithographically confined DNA origami. *Nature nanotechnology* **2010**, *5*, 121-126.

[6] Rothemund, P. W. Folding DNA to create nanoscale shapes and patterns. *Nature* **2006**, *440*, 297-302.

[7] Mignuzzi, S.; Pollard, A. J.; Bonini, N.; Brennan, B.; Gilmore, I. S.; Pimenta, M. A.; Richards, D.; Roy, D. Effect of disorder on Raman scattering of single-layer Mo S 2. *Physical Review B* **2015**, *91*, 195411.

[8] Berkdemir, A.; Gutiérrez, H. R.; Botello-Méndez, A. R.; Perea-López, N.; Elías, A. L.; Chia, C.-I.; Wang, B.; Crespi, V. H.; López-Urías, F.; Charlier, J.-C. Identification of individual and few layers of WS2 using Raman Spectroscopy. *Scientific reports* **2013**, *3*, 1755.

[9] Giannozzi, P.; Baroni, S.; Bonini, N.; Calandra, M.; Car, R.; Cavazzoni, C.; Ceresoli, D.; Chiarotti, G. L.; Cococcioni, M.; Dabo, I. QUANTUM ESPRESSO: a modular and open-source software project for quantum simulations of materials. *Journal of physics: Condensed matter* **2009**, *21*, 395502.

[10] van Setten, M. J.; Giantomassi, M.; Bousquet, E.; Verstraete, M. J.; Hamann, D. R.; Gonze, X.; Rignanese, G.-M. The PseudoDojo: Training and grading a 85 element optimized norm-conserving pseudopotential table. *Computer Physics Communications* **2018**, *226*, 39-54.

[11] Hinuma, Y.; Pizzi, G.; Kumagai, Y.; Oba, F.; Tanaka, I. Band structure diagram paths based on crystallography. *Computational Materials Science* **2017**, *128*, 140-184.

[12] Togo, A.; Tanaka, I. $\texttt {Spglib} $: a software library for crystal symmetry search. *arXiv preprint arXiv:1808.01590* **2018**.

[13] Rydberg, H.; Dion, M.; Jacobson, N.; Schröder, E.; Hyldgaard, P.; Simak, S.; Langreth, D. C.; Lundqvist, B. I. Van der Waals density functional for layered structures. *Physical review letters* **2003**, *91*, 126402.

[14] Grimme, S. Semiempirical GGA‐type density functional constructed with a long‐range dispersion correction. *Journal of computational chemistry* **2006**, *27*, 1787-1799.

[15] Zhang, X.; Rahman, M.; Neff, D.; Norton, M. L. DNA origami deposition on native and passivated molybdenum disulfide substrates. *Beilstein Journal of Nanotechnology* **2014**, *5*, 501-506.